

Propagation and Structure of Streamers in Liquid Dielectrics

Key Words: Streamer pattern, propagation mode and velocity, pre-breakdown mechanisms

by
The Liquid Dielectrics Committee International
Study Group, IEEE Dielectrics and Electrical
Insulation Society

A. BEROUAL, M. ZAHN, A. BADENT, K. KIST,
A.J. SCHWABE, H. YAMASHITA, K. YAMAZAWA,
M. DANIKAS, W.G. CHADBAND, AND Y. TORSHIN

The molecular structure has a significant effect on streamer propagation. The main parameter affecting propagation is the electronic affinity of the liquid molecules.

INTRODUCTION

The study of pre-breakdown and breakdown phenomena in liquid dielectrics has been the subject of many research investigations during the past three decades. Our understanding has been greatly improved by the use of fast digitizing oscilloscopes for voltage and current measurements; fast optical detecting systems for measurements of density gradients using shadowgraph and Schlieren photography, coupled with an image converter camera; electric field distributions using electric field induced birefringence of the Kerr effect; and optical spectroscopy of emitted light. These methods have revealed a lot of information about the processes occurring in the electrical breakdown of a dielectric liquid. Thus, it is possible to follow the different stages leading to breakdown and to establish that the breakdown of liquids is generally preceded by some events called “streamers,” where the optical refractive index is different from that of the surrounding liquid and the structure is similar to that observed in the breakdowns of gas and solid insulation. Con-

trary to the discharges in gases, the term “streamer” in liquid dielectrics also includes other structures, such as mono-channel patterns.

These streamers are characterized by different structures according to the experimental conditions. They produce typical shapes of current transients or emitted light signals. They are accompanied by shock waves and their conductivity depends on the mechanisms involved in their propagation. The streamer stops when the electric field becomes too small, producing a string of micro-bubbles that dissolve in the liquid. Note that Kerr effect measurements of the electric field found that streamers were highly conducting, with a voltage drop across the streamer that was <10% of the total voltage across the electrodes [1].

Streamers are generally classified as slow and “bushy” for streamers emanating from the negative electrode, or fast and “filamentary” for streamers emanating from the positive electrode. Positive streamers are often (about ten times) faster than negative streamers, although transformer oil is an exception, with positive and negative streamer velocities in the same range. According to recent work, streamers can be classified in different modes (1st, 2nd, 3rd, and even 4th) depending on their velocity and the polarity of the voltage [1]. Each propagation mode corresponds to a given inception electric field. Therefore, the electrode geometry and the amplitude of the applied voltage have a significant influence on the structure, the velocity, and the mode of propagation of the streamers. However, such a classification versus the polarity is inconclusive when considering liquids of specific molecular structure or containing selective additives.

The characteristics (structure, velocity, current...) of these streamers depend on the chemical composition and physical properties of the liquid (pure or containing a small concentration of selected additives); pressure and temperature; the electrode geometry; the voltage magnitude, polarity, and shape; and contaminants of air, moisture, particles, and other trace impurities.

Generally, measurements use contoured parallel plane electrodes for uniform electric field studies. Rod-plane and point-plane electrodes are used to localize the discharge initiation near the point using the field enhancement near the

point to initiate breakdown at modest voltages. The use of a point-to-point electrode geometry permits simultaneous observation of positive and negative streamers. Typical voltage waveforms are standard lightning impulses (1.2/50 μ s), impulses with short risetimes (<200ns), rectangular pulsed voltages, decaying oscillating waveforms (<100 kHz-1 MHz), and power frequency ac voltages (50 or 60 Hz).

Our purpose is to present a critical review of the current understanding of streamer propagation in liquids in order to help define the direction of future research.

POLARITY EFFECT ON STRUCTURE AND VELOCITY OF STREAMERS

The polarity effect in insulating oil in inhomogeneous electric fields manifests differences in the generation, structure, and propagation velocity of negative and positive streamers. Moreover, both classes of streamers pass through several typical propagation stages (or modes) on their way towards the counter electrode. Due to the different propagation velocities and patterns, the positive streamer can be classified in three consecutive stages: primary, secondary, and tertiary streamers. In contrast, the negative streamer shows only two propagation stages [2]. The appearance of each structure depends on the field inception.

Positive Streamers

When increasing the voltage, one can first observe the formation of positive primary streamers (PPS, or 1st mode) exhibiting an intensified branching. The streamer appears in an umbrella-like structure propagating with a constant velocity ranging from 2 to 3 km/s. The inception field of the PPS was determined to be $E_{i,pr+} > 2.0$ MV/cm. Just before contacting the opposite electrode, very fast events bridge the remaining gap and initiate breakdown.

Higher voltage levels lead to a reduced time to breakdown and to the formation of a positive secondary streamer (PSS, or 2nd mode) as an extension of the primary structure area with the highest branching. The inception field of a PSS refers to specific field strengths $E_{i,sec+} > 12$ MV/cm. Secondary streamers propagate with a significant higher velocity that can reach 32 km/s. They have a complex spatial structure in the form of a bright main channel with a radius of the order 60-90 μ m, bright lateral stems with a top zone of ionization in the shape of brush-type structures with a 0.7-1.2 mm radius, consisting of not less than 20 weak luminous streamers with a radius of 3-6 μ m (Fig. 1) [3]. At the streamer fronts, the shock waves are recorded.

Like slow positive streamers, fast positive streamers extend by jumps through a zone of ionization, accompanied by a streamer flash and by an increase of the ionization current at the moment of flash up to 0.05-0.5 A. The frequency of flashes increases with the average field E_a (E_a is the ratio between the applied voltage to the electrode gap). For $E_a = 55$ kV/cm, this frequency is about 1 MHz and the minimum

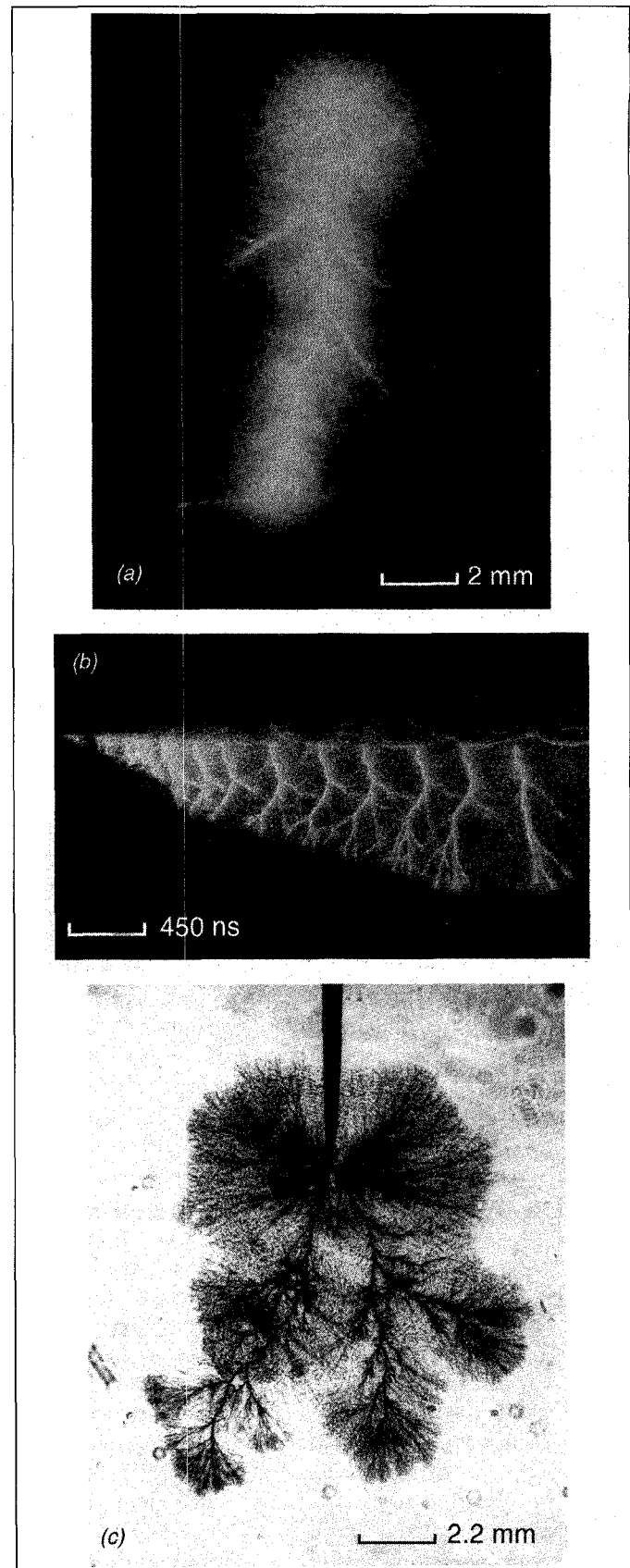


Fig. 1 Propagation of fast positive streamer in transformer oil in a point-plane electrode geometry under 0.5/85 μ s impulse voltage. Gap length 27.5 mm. Tip radius 30 μ m; Crest voltage 178 kV. (a) Still photograph (frame exposition 1 μ s), (b) Streak photograph, (c) Schlieren photograph (frame exposition 8 ns) [3].

density of the current is $\sim 1 \text{ kA/cm}^2$. The average field within a fast streamer ranges from 1.7 to 5 kV/cm; the number of electrons is $\sim 3 \times 10^{16} \text{ cm}^{-3}$ and the conductivity is $\sim 1 \text{ S/m}$.

Highly overstressing the gap causes a short primary streamer growth, an earlier secondary streamer inception, and an ultra-high speed tertiary streamer (PTS, or 3rd mode), which is often self-luminous. Only minor differences in structure between secondary and tertiary streamers could be observed. The tertiary streamer is less branched and often filamentary. Its velocity can exceed 100 km/s. For pulses with very short risetimes, the fast events dominate the pre-breakdown period and breakdown is initiated at an early time.

Negative Streamers

The negative streamer appears in two consecutive stages (or modes): primary and secondary streamers. Depending on the electric field the negative primary streamer (NPS, or 1st mode) shows different patterns. The NPS starts typically at fields: $E_{i,pr} > 2.5 \text{ MV/cm}$. At low fields the negative streamer structures resemble the shape of a leafless treetop, i.e., the streamer branches propagate both in paraxial and lateral directions and bridge the complete gap. The diameter of the streamer branches was determined to be approximately 30 to 70 μm , and the paraxial propagation velocity was approximately 1 km/s. Further, main streamer branches can obstruct progress and sometimes even suppress the growth of smaller side streamers. A further increase of the electrical field leads to an intensified branching of the streamer structure and increased streamer speed.

At higher fields the streamer appears as a compact bushy structure with many branches, propagating with velocities of about 1 to 3.5 km/s. At very high fields, the streamer shape changes again. Only one branch bridges the gap with a velocity that can exceed 100 km/s. For larger gaps ($> 40 \text{ mm}$), a secondary stage could be detected. Depending on the electric field, the negative secondary streamer structure (NSS, or 2nd mode) also develops in various patterns.

RF-Voltage Tests

Positive and negative streamers are formed alternately when the streamer inception voltage is exceeded. Depending on the growth rate of the electric field, all consecutive propagation stages (modes) can occur, i.e., in the case of negative polarity, primary and secondary streamers, and in the case of positive polarity, even a tertiary streamer. For cosine waveforms with frequencies up to 1 MHz, a positive primary streamer starts and propagates towards the counter electrode. When the voltage falls below the extinction voltage, the streamer stops. Further, its brightness decays and faint branches disappear. As soon as the voltage crosses zero, a negative structure is formed at the tip of the former positive streamer, which simultaneously changes into a negative streamer.

During propagation, the streamer pattern changes due to the alternate polarity of the consecutive half waves: (i) straight branches of the umbrella-like positive primary streamers disappear and several main branches are gener-

ated; (ii) at the tips of bush-like negative primary streamers, umbrella-like structures occur. At higher frequencies, the conversion from one polarity to the other requires a finite time, i.e., new streamer patterns cannot occur until all charge carriers of opposite polarity have been removed.

ELECTRICAL CURRENT AND LIGHT EMISSION

Transient current pulses are generally accompanied by light emission pulses. The current signal is often measured through the medium of the voltage across a non-inductive resistor in series with the test cell or by using optoelectronic techniques. The light emitted by streamers is detected by a photomultiplier tube or some other optical detector (e.g., a fast photodiode).

The amplitude and the shape of the streamer current and the corresponding emitted light in liquid dielectrics depend on many parameters. For small gaps ($< 5 \text{ cm}$) these currents are weak (no more than a few mA) and their shape depends on the polarity of the sharp electrode. In a point-plane electrode geometry, the current of a slow bushlike-negative streamer consists of bursts ($< 10 \text{ ns}$), irregularly spaced, with an amplitude that generally increases with time throughout the streamer propagation. The light, which is emitted across the entire gap, has a similar shape to that of the current. The number and amplitude of both streamer current and emitted light pulses increase when the voltage is increased for a given liquid [4-6].

The light emitted by the fast filamentary-positive streamer consists of a unique pulse, the current having a dc component [4, 5-9] on which are superimposed other pulses, much more regular than with a negative streamer. The current increases continuously to a maximum value generally attributed to the time at which the streamer reaches the insulating sheet covering the opposite electrode.

For both streamer polarities, the amplitude of the current and the intensity of the emitted light increase with the propagation velocity of the streamers. The currents of fast streamers are always higher than those of the slow ones, whatever the polarity and the tested liquids.

For long gaps (5 to 100 cm), both positive and negative streamer currents consist of irregularly spaced pulses [10]. With a rod-plane geometry, these pulses can reach a few amperes for a 100 cm gap. The current and emitted light waveforms of both negative and positive streamers under ac voltages are similar to those observed under impulse or step voltages.

As for the current, the spatial distribution and amplitude of the electrical charge in positive and negative streamers depend on the shape and velocity of the streamers themselves. The total electrical charge of fast positive and negative streamers is higher than that of the slow ones. Moreover, the larger the electrode gap and/or the point radius and/or the lower the voltage, the lower the streamer velocity and the lower the total charge. The more energetic the streamer, the higher its velocity.

Table I: Negative Streamer

Liquids	Ndl	Tip Radius	Gap Length	Voltage Waveform	kV	v_{max} / v_{av} km/s / km/s	Structure	Methods	Ref.
n-pentane	W	20 μ m	4 mm	2.3/1500 μ s	-45.9	0.40 / 0.07	bush	Schn, ICC	1
n-hexane	W	20 μ m	4 mm	2.3/1500 μ s	-48.1	0.60 / 0.11	bush	Schn, ICC	1,2
n-heptane	W	20 μ m	4 mm	2.3/1500 μ s	-48.1	0.50 / 0.13	bush	Schn, ICC	1
n-octane	W	20 μ m	4 mm	2.3/1500 μ s	-48.1	0.77 / 0.14	bush	Schn, ICC	1
n-nonane	W	20 μ m	4 mm	2.3/1500 μ s	-48.1	0.67 / 0.14	bush	Schn, ICC	1
n-decane	W	20 μ m	4 mm	2.3/1500 μ s	-50.4	0.75 / 0.16	bush	Schn, ICC	1
n-hexane (5 MPa)	Stl	35 μ m	2.3 mm	4 / 3 / 4 μ s	-156	/ 2.50	tree	SG, ICC	3
n-hexane (+2% IMN)	W	10 μ m	10 mm	1.1/225 μ s	-45.0	0.22 / 0.20	bush	Schn, ICC	4
n-hexane (+2% CCl ₄)	W	10 μ m	10 mm	1.1/225 μ s	-45.0	0.91 / 0.48	filament	Schn, ICC	4
cyclo-hexane	W	20 μ m	4 mm	2.3/1500 μ s	-52.7	0.35 / 0.17	bush	Schn, ICC	2
cyclo-hexane (initiation)	W	0.5 μ m	4.7 mm	0.2/540 μ s	-5.30 -6.18 -7.95 -9.71	0.037 / 0.014 0.043 / 0.013 0.057 / 0.019 0.051 / 0.021	sphere hemi-sph pagoda bush	SG, ICC	5,6
c-hexane (+0.2% anthracene)	Stl	3 μ m	4 mm	0.4 μ s step	-50.0	/ 0.19	bush	SG, VCR	7
c-hexane (+1% CCl ₄)	Stl	3 μ m	4 mm	0.4 μ s step	-50.0	/ 0.64	tree	SG, VCR	7
CCl ₄	W	10 μ m	4 mm	2.2/190 μ s	-42.8	/ 8.40	tree	Schn, ICC	8
2-methyl-pentane	W	20 μ m	4 mm	2.3/1500 μ s	-48.1	0.48 / 0.18	bush	Schn, ICC	9
2,3-dimethyl-butane	W	20 μ m	4 mm	2.3/1500 μ s	-48.1	0.24 / 0.16	bush	Schn, ICC	9
iso-octane	Stl	35 μ m	20mm	4 / 3 / 4 μ s	-47.0	/ 0.26	bush	SG, ICC	10
benzene	W	20 μ m	4 mm	2.3/1500 μ s	-50.4	0.42 / 0.19 0.86 / 0.27	bush tree	Schn, ICC	2
benzene (+1% CCl ₄)	W	few μ	4 mm	15ns/4 μ s	-40.0	/ 1.30	tree	Schn, ICC	11
monochloro-benzene	W	10 μ m	4 mm	2.2/190 μ s	-42.8	/ 0.45	bush	Schn, ICC	8
toluene	Stl	35 μ m	10 mm	4 / 3 / 4 μ s	-40.0	0.27 / 0.17	bush	SG, ICC	12
toluene (5 MPa)	Stl	35 μ m	2.5 mm	4 / 3 / 4 μ s	-100	/ 4.50	tree	Schn, ICC	13
1-hexene	W	20 μ m	4 mm	2.3/1500 μ s	-48.1	0.21 / 0.14	bush	Schn, ICC	2
1,5-hexadien	W	20 μ m	4 mm	2.3/1500 μ s	-48.1	0.32 / 0.27	bush	Schn, ICC	9
cyclo-hexene	W	20 μ m	4 mm	2.3/1500 μ s	-39.0	3.27 / 1.08	tree	Schn, ICC	9
H ₂ O (2 - 20.3 M Ω .cm)	W	20 μ m	4 mm	2.3/1500 μ s	-16.2	0.08 / 0.04 0.49 / 0.20 1.78 / 0.60	sphere bush tree	Schn, ICC	9
L-Helium	W	20 μ m	4 mm	2.3/1500 μ s	-30.0	7.05 / 3.97	filament	Schn, ICC	9
L-Nitrogen	W	20 μ m	4 mm	2.3/1500 μ s	-43.1	0.23 / 0.13	bush	Schn, ICC	9
L-Nitrogen (initiation)	W	1 μ m	5 mm	0.2/540 μ s	-17.6 -17.6	0.10 / 0.06 0.40 / 0.12	bush filament	SG, ICC	14
PFPE	Stl	35 μ m	5 mm	4 / 3 / 4 μ s	-49.0	/ 4.50	tree	SG, ICC	15
PFPE (initiation)	W	1 μ m	5 mm	0.2/540 μ s	-21.2 -33.6	0.35 / 0.21 3.29 / 1.35	bush filament	SG, ICC	16
Si-Oil (10 cSt)	W	8 μ m	1.4 mm	2 μ s pulse 30 μ s pulse	-22.0	/ 0.04 / 0.06	bush tree	SG, SS	17
TFO	W	20 μ m	4 mm	2.3/1500 μ s	-35.7	2.07 / 0.76 3.38 / 1.47	bush tree	Schn, ICC	18
TFO (naphthenic)	Cu	0.6 mm	67 mm	1/180 μ s	-343	50.0 / 16.0	tree	LE, ICC	19
White-Oil (naphthenic)	Stl	35 μ m	10 mm	4 / 3 / 4 μ s	-53.0	/ 0.20	bush	SG, ICC	10

IMN:1-methylnaphthalene W:tungsten
 PFPE:perfluoro-polyether Stl:steel
 TFO:transformer oil Cu:copper

v_{max} :maximum speed
 v_{av} :average speed

Schn:Schlieren
 SG:shadowgraph
 LE:light emission
 SS:single shot

ICC:Image Converter Camera
 VCR:video recorder

Table II: Positive Streamer

Liquids	Ndl mat	Tip Radius	Gap Length	Voltage Waveform	kV	v_{max} / v_{av} km/s / km/s	Structure	Methods	Ref.
n-pentane	W	20 μ m	4 mm	2.3/1500 μ s	+30.9 +40.4	0.52 / 0.23 6.97 / 4.23	bush tree	Schn, ICC	1
n-hexane	W	20 μ m	4 mm	2.3/1500 μ s	+32.7 +45.1	0.48 / 0.21 7.61 / 3.86	bush tree	Schn, ICC	1,2
n-heptane	W	20 μ m	4 mm	2.3/1500 μ s	+42.8	6.32 / 4.04	tree	Schn, ICC	1
n-octane	W	20 μ m	4 mm	2.3/1500 μ s	+48.7	6.20 / 5.17	tree	Schn, ICC	1
n-nonane	W	20 μ m	4 mm	2.3/1500 μ s	+47.5	6.67 / 4.28	tree	Schn, ICC	1
n-decane	W	20 μ m	4 mm	2.3/1500 μ s	+52.3	7.48 / 5.15	tree	Schn, ICC	1
dodecane	W	1 μ m	2.5 mm	10/632 ns	+25.0	6.00 / 3.09	tree	SG, SS	20
hexadecane	W	1 μ m	2.5 mm	10/632 ns	+24.0	4.00 / 2.70	tree	SG, SS	20
squalane	W	1 μ m	2.5 mm	10/632 ns	+25.0	4.00 / 2.06	tree	SG, SS	20
n-hexane (5 MPa)	Stl	35 μ m	3.5 mm	4 / 3 / 4 μ s	+117	/ >18.0	filament	SG, ICC	3
n-hexane (+0.1% 1MN)	W	10 μ m	10 mm	1.1/225 μ s	+45.1	/ 3.19	tree	Schn, ICC	4
n-hexane (+5% DMA)	W	10 μ m	10 mm	1.1/225 μ s	+45.1	/ 2.78	radial	Schn, ICC	4
cyclo-hexane	W	20 μ m	4 mm	0.2/540 μ s	+45.1	0.33 / 0.24 3.22 / 2.54	bush tree	Schn, ICC	2
cyclo-hexane (initiation)	W	0.5 μ m	4.7 mm	0.12/830 μ s	+8.5 +29.1	0.22 / 0.13 2.85 / 1.53	bush filament	SG, ICC	5,6
c-hexane (+0.98mol NB)	W	1 μ m	4 mm	50ns/2 ms	+35.0	/ 4.90	filament	LE, VCR	21
c-hexane (+0.49mol TCE)	W	1 μ m	4 mm	50ns/2 ms	+35.0	/ 1.60	filament	LE, VCR	21
CCl ₄	W	10 μ m	4 mm	2.2/190 μ s	+42.8	/ 30.00	tree	Schn, ICC	8
2-methyl-pentane	W	20 μ m	4 mm	2.3/1500 μ s	+45.1	9.33 / 3.65	tree	Schn, ICC	9
2,3-dimethyl-butane	W	20 μ m	4 mm	2.3/1500 μ s	+45.1	5.59 / 4.14	tree	Schn, ICC	9
benzene	W	20 μ m	4 mm	2.3/1500 μ s	+45.1	1.68 / 1.47	radial	Schn, ICC	2
monochloro-benzene	W	10 μ m	4 mm	2.2/190 μ s	+42.8	/ 76.00	tree	Schn, ICC	9
trichloro-benzene	W	10 μ m	4 mm	2.2/190 μ s	+42.8	/ 62.00	tree	Schn, ICC	8
dodecyl-benzene	W	10 μ m	4 mm	2.2/190 μ s	+42.8	/ 2.30	tree	Schn, ICC	8
iodo-benzene	W	10 μ m	4 mm	2.2/190 μ s	+42.8	/ 15.00	tree	Schn, ICC	8
toluene (5.0 MPa)	Stl	35 μ m	2.5 mm	4 / 3 / 4 μ s	+123	/ >25.0	tree	Schn, ICC	13
1-hexene	W	20 μ m	4 mm	2.3/1500 μ s	+45.1	4.51 / 2.92	tree	Schn, ICC	2
1,5-hexadiene	W	20 μ m	4 mm	2.3/1500 μ s	+45.1	15.21 / 6.49	tree	Schn, ICC	9
cyclo-hexene	W	20 μ m	4 mm	2.3/1500 μ s	+45.1	8.81 / 4.36	tree	Schn, ICC	9
DOP	W	1 μ m	4 mm	50ns/2 ms	+21.0	/ 0.90	filament	LE, SS	21
DOP (+2.84mol AN)	W	1 μ m	4 mm	50ns/2 ms	+22.0	/ 1.00	filament	LE, SS	21
H ₂ O (2 · 20.2 M Ω .cm)	W	20 μ m	4 mm	2.3/1500 μ s	+28.5	2.73 / 0.04 45.30 / 26.70	bush tree	Schn, ICC	9
L-Helium	W	20 μ m	2.2 mm	1/1600 μ s	+42.0	0.33 / 0.02	sphere	Schn, ICC	9
L-Nitrogen	W	20 μ m	4 mm	1/1600 μ s	+39.6	0.31 / 0.12 29.60 / 18.70	bush tree	Schn, ICC	9
L-Nitrogen (initiation)	W	1 μ m	5 mm	0.2/540 μ s	+17.6 +17.6	0.18 / 0.05 1.34 / 0.13	bush filament	SG, ICC	14
PFPE	Stl	35 μ m	5 mm	4 / 3 / 4 μ s	+65.0	/ 30.00	tree	SG, ICC	15
PFPE (initiation)	W	1 μ m	5 mm	0.2/540 μ s	+20.3 +24.7	0.37 / 0.18 8.21 / 1.46	bush filament	SG, ICC	16
Si-Oil (100 cSt)	W	10 μ m	1.2 mm	450ns pulse	+10.9	/ 2.00	tree	SG, SS	17
TFO	W	20 μ m	4 mm	2.3/1500 μ s	+43.3	5.00 / 2.50	radial	Schn, ICC	18
TFO (naphthenic)	Cu	0.6mm	67 mm	1/180 μ s	+327	17.80 / 4.96 210.00 / 65.00	bush filament	LE, ICC	19
White-Oil (naphthenic)	Stl	3 μ m	25.4 mm	1/2500 μ s	+63.0	1.80 / 1.07	tree	Schn, SS	22

1MN:1-methylnaphthalene W:tungsten
 DMA:N,N'-dimethylaniline Stl:steel
 NB:nitrobenzene Cu:copper
 TCE:tetra-chloroethylene
 DOP:di-octylphthalate
 AN:acetonitril
 PFPE:perfluoro-polyether
 TFO:transformer oil

v_{max} :maximum velocity Schn:Schlieren
 v_{av} :mean velocity SG:shadowgraph
 LE:light emission
 SS:single shot
 ICC:Image Converter Camera
 VCR:video camera

INFLUENCE OF LIQUID STRUCTURE

The molecular structure has a significant effect on the streamer propagation. The main parameter affecting streamer propagation is the electronic affinity of the liquid molecules. In halogenated liquids, the positive and negative streamer velocities are very important compared with those in liquids without halogens (Tables I and II). The presence of a single atom of chlorine in chlorocyclohexane leads to a large increase in the negative streamer velocity, about ten

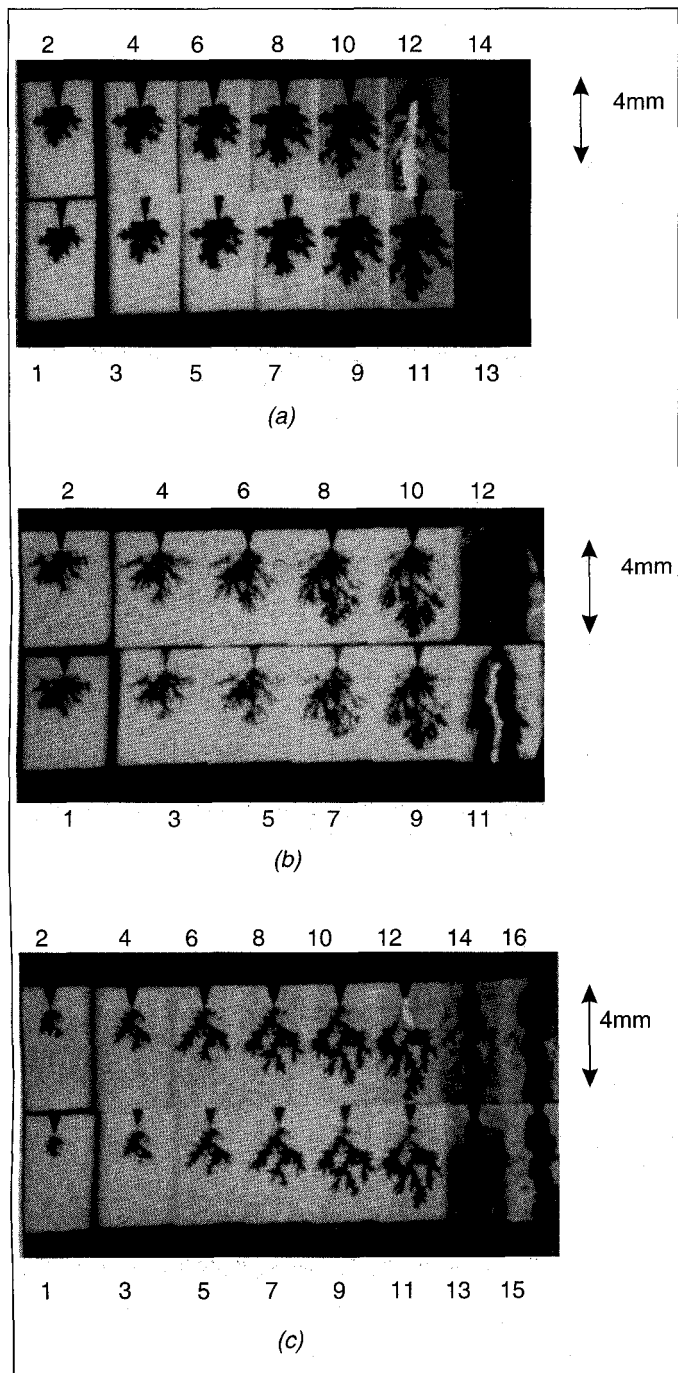


Fig. 2 Negative bush-like streamers in saturated hydrocarbon liquids. Gap length 4 mm; Tip radius $20\ \mu\text{m}$. (a) n-pentane: - 45.9 kV, $2\ \mu\text{s}/\text{Frame}$; (b) n-heptane: - 48.1 kV, $2\ \mu\text{s}/\text{Frame}$; (c) n-decane: - 50.4 kV; $2\ \mu\text{s}/\text{Frame}$ [14].

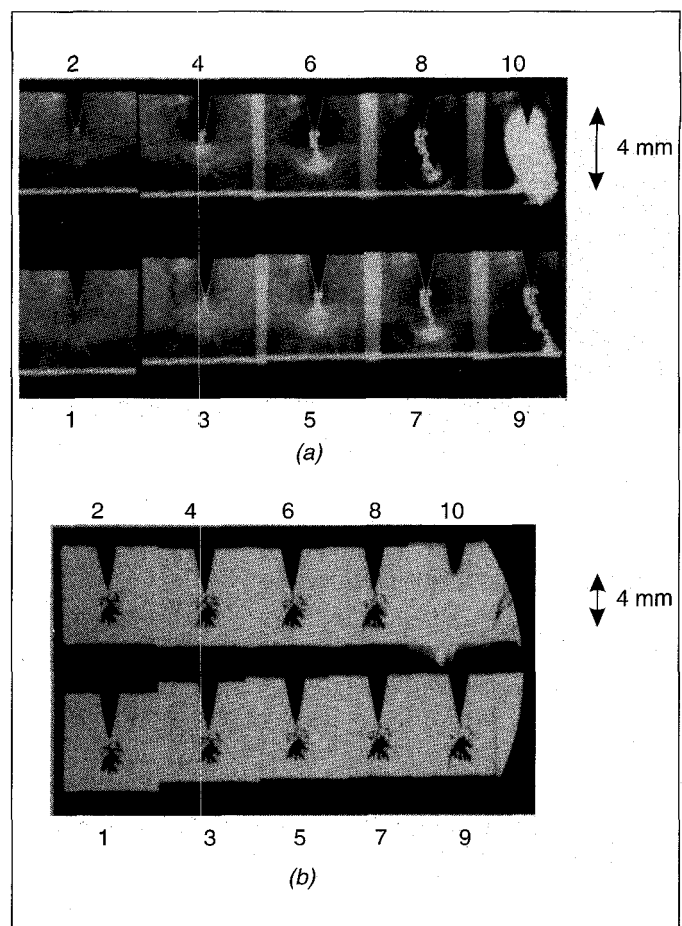


Fig. 3 Streamer structures in benzene. Gap length 4 mm; Tip radius $20\ \mu\text{m}$. (a) tree-like: - 45.1 kV, $1\ \mu\text{s}/\text{Frame}$. (b) bush-like: - 51.5 kV, $1\ \mu\text{s}/\text{Frame}$ [14].

times that of cyclohexane [5]. When the point is positive, the streamer is much more filamentary in chlorocyclohexane than in other liquids such as cyclohexane, transdecahydronaphthalene and cis-decahydronaphthalene.

In most saturated hydrocarbon liquids and with larger tip radii ($> 10\ \mu\text{m}$), the negative streamer has a bush-like structure (Fig. 2), whereas in pure aromatics (unsaturated hydrocarbon) liquids, a tree-like structure can also appear (Fig. 3). A negative filamentary streamer has been observed in liquid helium and in liquid nitrogen. Figure 4 shows a positive streamer having a radial structure in benzene.

Investigation of a number of silicone fluids of identical chemical nature but with viscosity varying from 10 to 10,000 cSt found no significant change of streamer velocity or shape [11]. Similar results, including no significant change in time to breakdown, have been found for polydimethylsiloxanes, also varying by a factor of 1000 in viscosity. These results indicate that viscosity has little effect on the breakdown process.

Other work found similar expansion rates of shock waves resulting from breakdown in liquids of differing viscosity, such as n-hexane, isooctane, cyclohexane, and toluene [12]. It is difficult to find a simple relation between mass density and the streamer velocity.

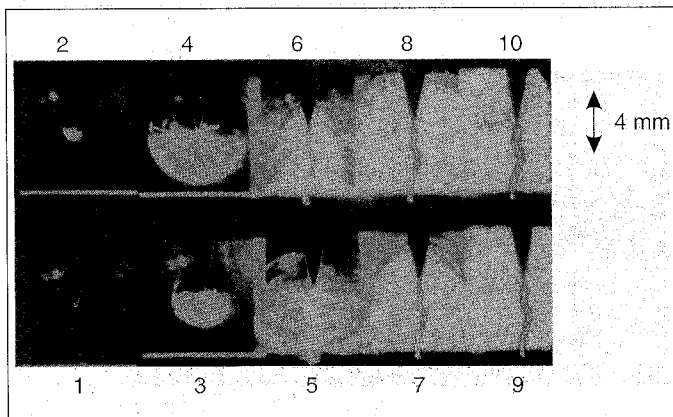


Fig. 4 Positive radial streamer in benzene. Gap length 4 mm; Tip radius 20 μm ; + 50.4 kV, 1 $\mu\text{s}/\text{Frame}$ [14].

EFFECTS OF ELECTRODE GEOMETRY

The velocity and the mode of propagation of streamers depend enormously on the electric field, which in turn is a function of the applied voltage U , the electrode geometry (electrode radii and gap), and the space charge coming from the bulk of the liquid or injected.

The electric field E_0 at the point of a needle electrode plays an important role in the initiation phase of streamers. According to the value of this field, it could be possible to initiate different structures of streamers. Thus, if the radius of curvature of the electrode point (r_0) is sufficiently small, a modest voltage can give a large electric field at the needle tip. For impulse and ac voltages for $r_0 < 3 \mu\text{m}$, streamers initiate for $E_0 > 10 \text{ MV}/\text{cm}$ while for $r_0 > 100 \mu\text{m}$, streamers initiate when $E_0 > 1 \text{ MV}/\text{cm}$. E_0 is the field determined by assuming the electrode point to be a hyperboloid of revolution with no injected charge.

The streamer structure can change with the radius of the point electrode. For smaller tip radii ($< 1 \mu\text{m}$), the structure of a negative streamer in cyclohexane changes from spherical (a) to hemispherical (b), pagoda-like (c), and bush-like (d) with increasing applied voltage as shown in Fig. 5.

In highly divergent electrode geometries under ac fields with gaps $\sim 25 \text{ mm}$, with a mean field $E < 40 \text{ kV}/\text{cm}$, breakdown is controlled by the propagation of positive streamers, whereas in moderately divergent geometries with gaps $\sim 5 \text{ mm}$ and a mean field $E < 80 \text{ kV}/\text{cm}$, breakdown is controlled by negative streamers. The time to breakdown usually increases linearly with gap, while the amplitude, duration, number, and length of partial discharge streamers decrease with increasing gap.

EFFECTS OF HYDROSTATIC PRESSURE AND TEMPERATURE

As the hydrostatic pressure is increased, the electrical breakdown strength generally increases, the number and amplitude of current and light pulses are reduced, and the streamer shape and length decrease, tending to form a string of globules (Fig. 6) [13]. Above a threshold pressure that depends on streamer energy, the streamer, the corresponding

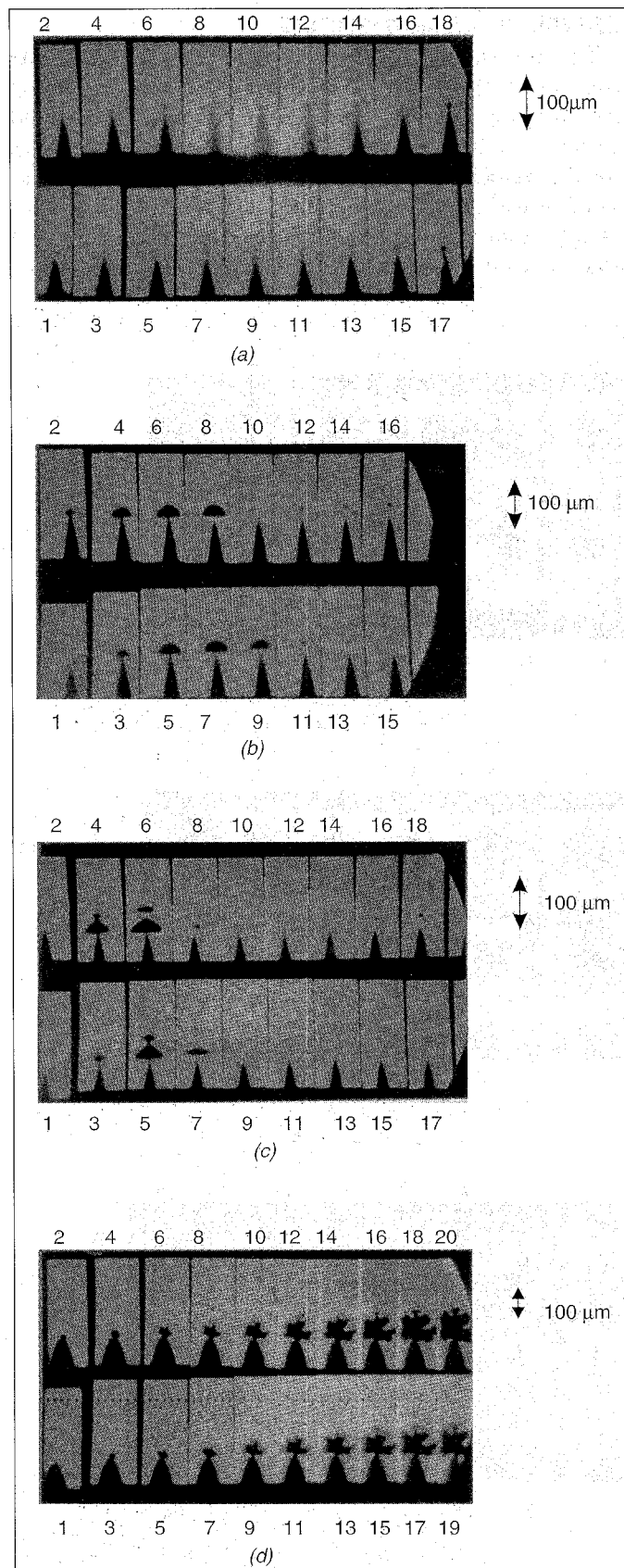


Fig. 5 Various streamer structures in cyclohexane. Gap length 5 mm; Tip radius 0.5 μm for (a)-(c), 15 μm for (d). (a) spherical: - 6.18 kV, 100 ns/Frame; (b) hemispherical: - 7.95 kV, 1 $\mu\text{s}/\text{Frame}$; (c) pagoda-like: - 7.95 kV, 1 $\mu\text{s}/\text{Frame}$; (d) bush-like: - 29.14 kV, 100 ns/Frame [14].

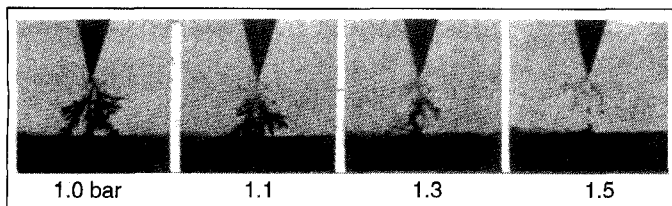


Fig. 6 Influence of hydrostatic pressure on the shape of the negative streamer in cyclohexane. Voltage 28 kV; Gap length 1 mm; Tip radius $5 \mu\text{m}$. All photographs are taken after $7 \mu\text{s}$ [18].

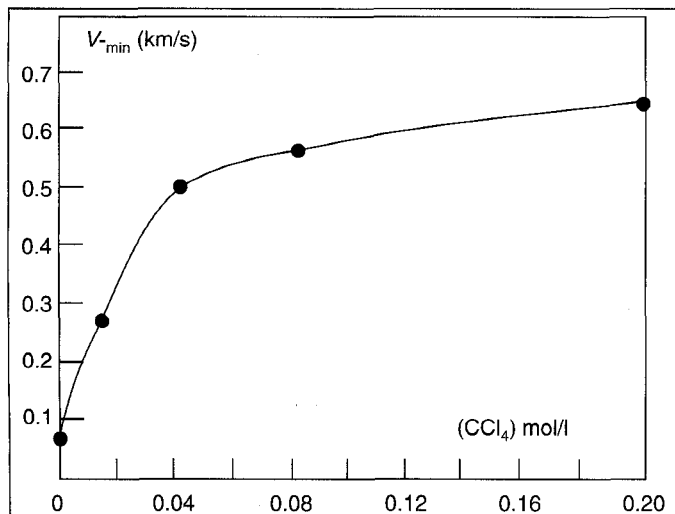


Fig. 7 Influence of CCl_4 concentration on the negative streamer velocities in cyclohexane under step voltage. Gap length 2 mm; Tip radius $3 \mu\text{m}$; Voltage 33 kV [13].

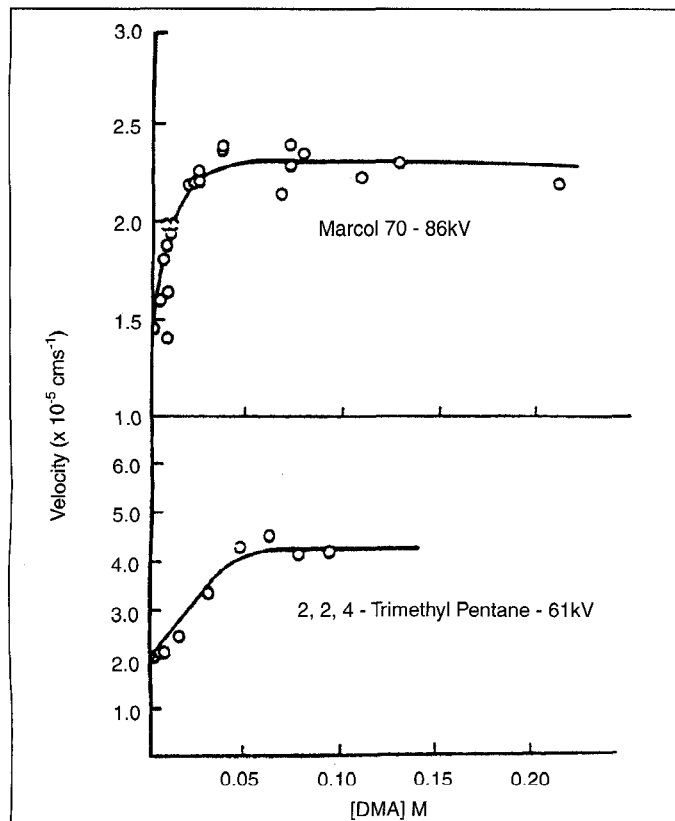


Fig. 8 Effect of DMA concentration on the positive streamer velocity in Marcol 70 and 2,2,4-trimethylpentane [6].

current, and light pulses disappear [11, 14]. The higher the amplitude and the number of the current (and the light) pulses, the higher is the hydrostatic pressure necessary to cause vanishing of the current pulses. No appreciable effect has been reported when reducing the pressure below atmosphere.

At atmospheric pressure, temperature has only minor effects on streamer behavior. The number and amplitude of current and light pulses from slow streamers increase with temperature while filamentary streamers are unaffected by temperature.

EFFECTS OF ADDITIVES

Small concentrations of polyaromatic compounds greatly reduce the impulse breakdown voltage of a naphthenic oil between a negative point and a grounded sphere [15]. This reduction in the breakdown voltage is due either to an increase of the streamer velocity or to the diminution of the initiation voltage. Since these compounds have both low ionization potentials and large electronic-trapping sections, it is difficult to distinguish the phase (initiation or propagation) that is affected by their presence. In pioneering work, Devins et al. [4] separately studied the influence of each property of additives (electronic scavenger or low ionization potential) and showed the importance of electronic processes. They observed that the addition of a non-ionic electronic scavenger such as sulfur hexafluoride (SF_6) or ethyl chloride ($\text{C}_2\text{H}_5\text{Cl}$), to a naphthenic oil or to 2,2,4-trimethylpentane renders the negative streamers more filamentary and increases their velocities [4]: With 0.05 mol/l of SF_6 or $\text{C}_2\text{H}_5\text{Cl}$, the streamer velocity can reach five times its initial value. There are no detectable effects on the positive streamers in these liquids. These results have been confirmed by others. By adding 0.04 mol/l of CCl_4 to cyclohexane, Beroual et al. [5] observed that the negative streamer velocities increase by a factor of 10. Above 0.04 mol/l, the increase of the velocity becomes less important (Fig. 7). There are no detectable additive effects on the positive streamers in these liquids.

The addition of a non-ionic low ionization potential compound such as N,N-dimethylaniline (DMA) does not change the negative streamer velocity, whereas it increases (by a factor of two to three) the positive streamer velocity in a naphthenic oil (Marcol 70) and in 2,2,4-trimethylpentane (Fig. 8). In both cases, there is a concentration (about 0.05 mol/l) above which no significant increase in the velocity is observed [4].

The addition of a low ionization potential compound (0.05 mol/l) such as tetramethyl paradiphenylamine (TMPD) (Fig. 9) to cyclohexane leads to a moderate increase of the negative streamer velocity (by a factor lower than two) and the shape of the streamer is practically unmodified [11]. The positive streamer velocity, under the same conditions, is multiplied by a factor of three and they become still more filamentary. A similar effect is observed with DMA [4, 16, 17]. The influence of electronic scavenger and low ionization potential compounds is comparable in other liquids,

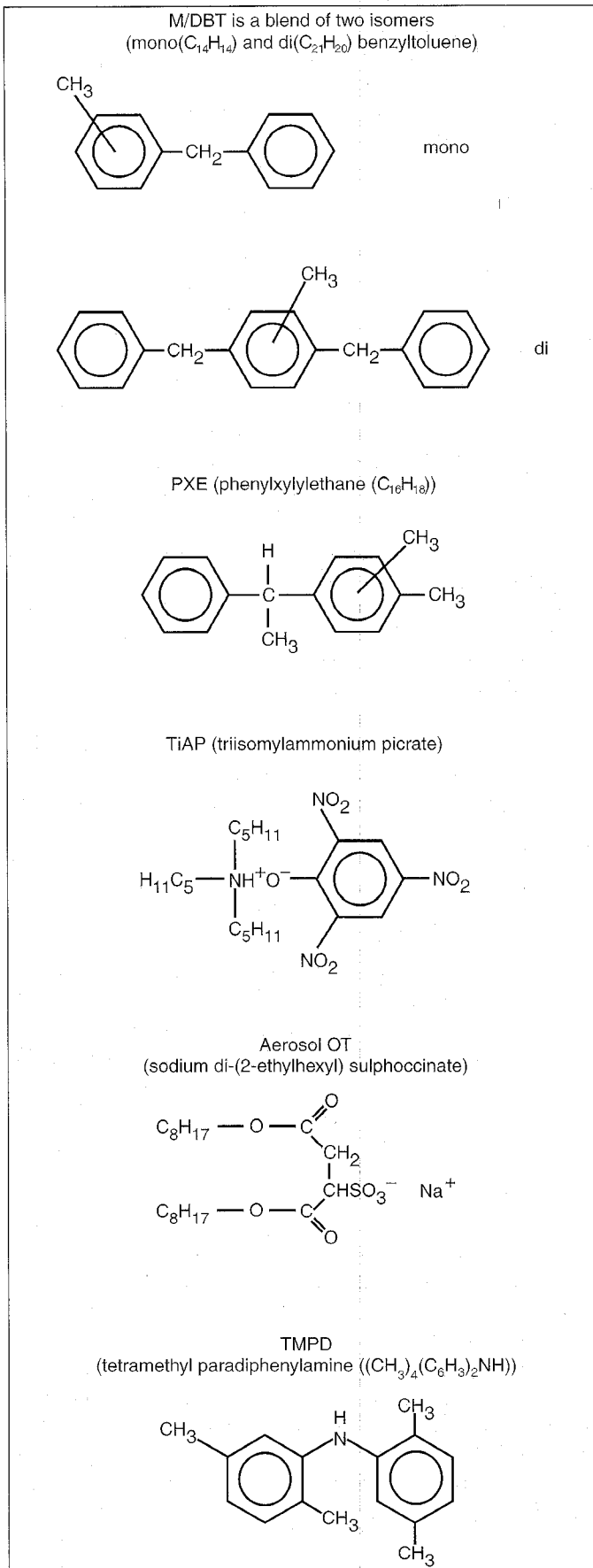


Fig. 9 Structure of oil components

such as phenylxylylene (PXE) and mono-dibenzyltoluene (M/DBT) [14], a blend of two isomers (mono($C_{14}H_{14}$) and di($C_{21}H_{20}$) benzyltoluene) (Fig. 9).

Ionic additives such as picrate of triisomyllammonium (TIAP) and Aerosol OT (Fig. 9) also have an influence on the streamer shape and velocity [11]. With a concentration of AOT comparable to that of CCl_4 in cyclohexane (typically about 10^{-1} mol/l), the velocity when the point is negative is multiplied by a factor of ten as in the case of CCl_4 .

Additives also change the shape and amplitude of currents for slow negative streamers. The number and amplitude of the current peaks increase when adding electronic scavenger additives such as CCl_4 [14]. A similar effect is observed in other liquids such as M/DBT and PXE.

SPECTRAL AND CHROMATOGRAPHIC ANALYSES

Spectroscopic studies of the light emitted during the pre-breakdown phase in liquid dielectrics extend from the UV to the visible range [18-20]. They revealed, in n-hexane, the presence of atomic and molecular hydrogen and carbon molecules (C_2 and C_3), and tiny amounts of metal emanating from the electrode metal. The formation of these species is attributed to an electron avalanche mechanism similar to that known to occur in gas discharges.

The spectra obtained in liquids such as cyclohexane (C_6H_{12}), a blend of mono- and dibenzyl toluene (M/DBT), and phenylxylylene (PXE) (Fig. 6), in a point-plane electrode system, reveal spectra lines (emerging from a continuum corresponding to molecular fragments) belonging to atomic as well as molecular hydrogen (H_2 line) and carbonaceous matter (C_2 Swan bands) resulting from the decomposition of the fluid (Figs. 10 and 11) [20]. These characteristic lines are more intense when the point is an anode than when it is a cathode. This parallels the fact that positive streamers are much more energetic than the negative ones.

The more energetic the streamer, that is, the faster it is, the more important the characteristic lines (H_γ and H_α lines, and C_2 Swan bands in this study) emerging from the basic envelope of the light emission spectrum. This indicates that the higher the streamer energy, the higher the possibility of the dissociation of the liquid molecules.

Results of chromatographic analysis of the dissolved gases generated by streamers in liquids such as PXE and M/DBT confirm those obtained with the spectroscopic analysis. The products revealed by chromatography are H_2 , CH_4 , C_2H_4 , C_2H_6 and C_2H_2 . Hydrogen and acetylene are mainly present and their quantities are much higher in positive polarity than in negative polarity for a given liquid [20]. These products are likely the results of the recombination of carbon and hydrogen resulting from the dissociation and fragmentation of liquid molecules.

Models and Discussion

The correlation observed between the shape and the velocity of the streamer, the corresponding current, and the associated light emission suggested an estimation method of

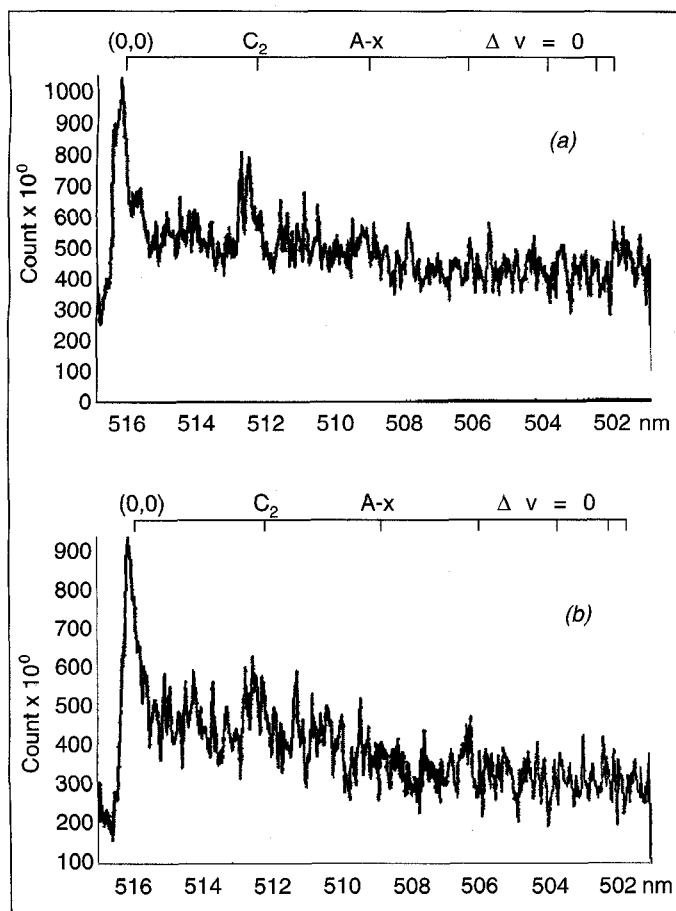


Fig. 10 Streamer spectra in cyclohexane under step voltage: Voltage $V = 32$ kV; Gap length $L = 0.5$ mm; Tip radius $r_p = 3 \mu\text{m}$. Central window of the spectrograph (dispersion 1.2 nm/mm) set at 509.3 nm: (a) fast positive streamers, (b) fast negative streamers. Accumulated data of about 100 streamers [23].

the current using simple models [21]. The slow bush-like streamer is assumed to be a conducting sphere growing from the point towards the plane, and the fast filamentary streamer is modeled as an extension of the point moving towards the opposite electrode. These models have been proposed elsewhere [5, 22, 23] to correlate the electric field to the streamer velocity. However, even though assuming the streamer as a conductor found some confirmation using Kerr effect measurements in nitrobenzene, one must be very careful when considering the shape of fast or slow streamers, since neither the shape nor the order of magnitude of the measured currents corresponds to either of these models. Moreover, currents corresponding to filamentary streamers are much higher than those of bushlike streamers, unlike those predicted by the above models. Consequently, these oversimplified physical representations are not very helpful in correlating the transient current and the velocity. It could be interesting to search other models and methods to evaluate the transient currents.

To explain the viscosity effect of liquids, Watson et al. [22] proposed a model in which the viscous drag is balanced by the electrostatic force at the streamer tip. This model has a viscosity limiting the growth of an electrohydrodynamic in-

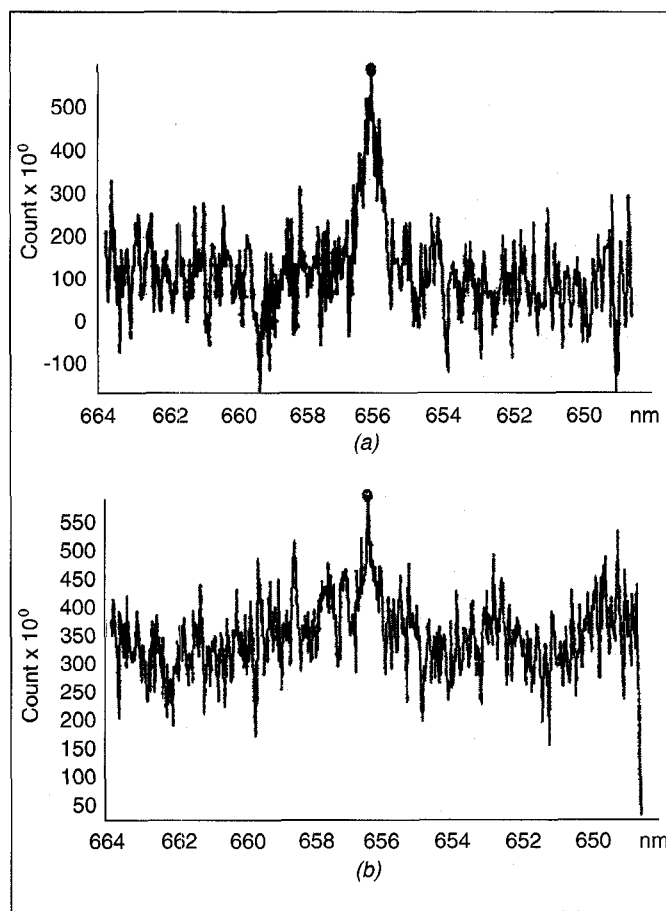


Fig. 11 Streamer spectra in cyclohexane under step voltage: Voltage $V = 32$ kV; Gap length $L = 0.5$ mm; Tip radius $r_p = 3 \mu\text{m}$. Central window of the spectrograph (dispersion 1.2 nm/mm) set at 656.3 nm: (a) positive streamers, (b) negative streamers [23].

stability driven by the electrical force on the streamer charge. This causes an initially spherical cavity to form a multi-branched structure. In supporting experiments [24], low viscosity liquids produce bushy negative streamers with numerous branches, while high viscosity liquids produce spheroidal shadows with few or no branches. The shape and growth rate of the experimentally observed streamers, in liquids of low and high viscosity, seem to be in a good accordance with the electrohydrodynamic instability model.

According to other investigators [11], the model proposed by Watson et al. [22] is somewhat in contradiction with the experimental results concerning the influence of the viscosity. Indeed, by varying the viscosity by three orders of magnitude (from 90 to 4×10^5 cSt at 20°C), no significant variation of the streamer velocities and their shape was observed. Therefore, the influence of the viscosity must be further investigated with additional experiments on different liquids.

In order to explain the influence of additives and the molecular structure of the liquid medium on streamer propagation, Devins et al. [4] proposed a model in which they assumed that field ionization occurs in the liquid. They used Zener's theory of tunneling in solids to calculate the concen-

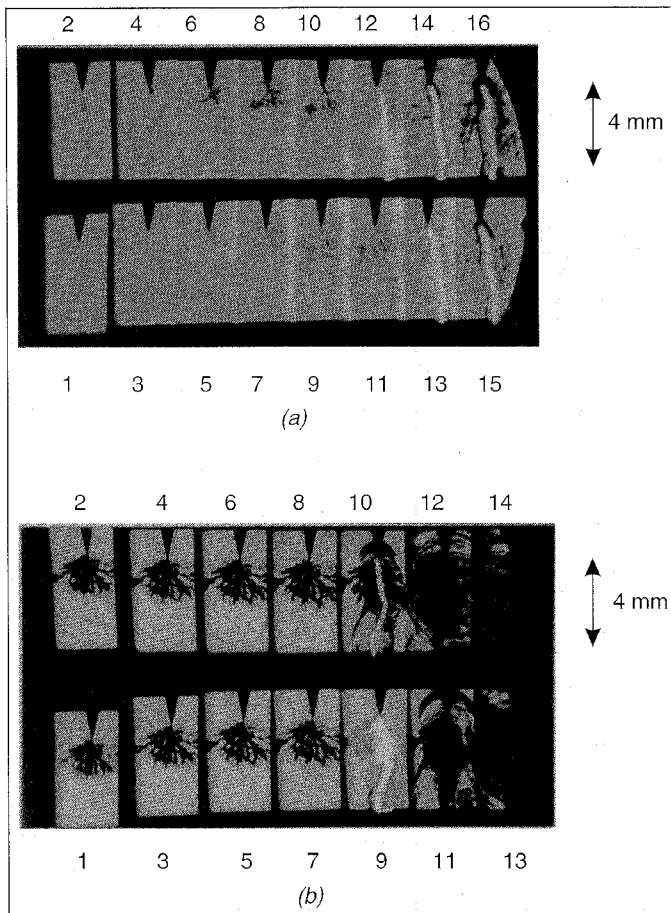


Fig. 12 Structures of positive streamers in n-pentane. Gap length 4 mm; Tip radius 20 μm . (a) tree-like: + 40.4 kV, 100 ns/Frame; (b) bush-like: + 30.9 kV, 500 ns/Frame [14].

tration of the positive and negative carriers contained in a cylindrical conducting channel. The propagation of negative streamers occurs in two stages: electron injection and trapping followed by ionization within the liquid. It results in a plasma similar to that produced when the point is positive. This model does not provide an evaluation of the time spent in each mode.

On the other hand, according to Devins et al. [4], the streamer velocity v increases when the mass density ρ decreases. This is in contradiction with the experimental results. Indeed, by considering two dielectric liquids having roughly the same mass density such as benzene ($\rho=0.8879 \text{ g/cm}^3$) and chlorobenzene ($\rho=1.107 \text{ g/cm}^3$), it has been observed that the positive streamer velocities v can be different: 1.2 and 76 km/s, respectively, in the same experimental conditions [19]. It seems difficult to find a simple relation between ρ and v . On the other hand, the model proposed by Devins et al. states that the velocity of positive streamers is constant, whereas it is not correct as shown experimentally by others [5, 23]. In spite of the contradictions discussed above, the model of Devins et al. is supported by two facts: (i) the addition of electronic scavengers reduces the trapping distance and the time t_1 spent in the first step, and thus increases the negative streamer velocity; (ii) the addition of

low ionization potential compounds increases the rate of ionization and reduces the time t_2 spent in the second step, and thus also increases the velocity. Further research needs to evaluate the times t_1 and t_2 .

In recent work, Beroual [14] has proposed a model explaining the relationship of the current and the corresponding electrical charge, the emitted light, the shape, and the velocity of streamers. This model, based on energetic considerations, explains the pre-breakdown processes that can occur, the propagation mode of streamers (i.e., by steps or continuous), and the influence of additives, and it evaluates the propagation velocity of the streamer. It is shown that the streamer that consists of irregularly spaced current bursts moves by jumps. The higher the frequency and amplitude of the current pulses, the shorter the duration between these steps and the higher the average velocity of the streamer. Then, the streamer tends to propagate continuously. This can be obtained by adding an electronic scavenger (to a slow negative streamer) or low ionization potential (to a fast positive streamer) compounds or yet by increasing the voltage (Fig. 12). The streamer velocity can exceed 100 km/s. On the other hand, the higher the elementary charge corresponding to each current pulse, then the more energetic the streamer, the higher will be its velocity and the more filamentary will be its shape. This model must be further completed by estimation of the local electrical charge at the streamer head during its propagation.

CONCLUSIONS

The streamer structure and its characteristics (velocity, current and emitted light, conductivity...) depend on many parameters, especially the chemical composition of the liquid (pure or containing selective additives); the applied voltage (shape, magnitude, and polarity); the electrode arrangement (gap length and electrode radius of curvature); and the hydrostatic pressure. Depending on the experimental conditions, different structures and propagation modes of streamers can be observed. The main parameters governing the streamer structure through the electrode gap (i.e., at each step of the streamer development) are the local electric field on the streamer tip, the average electric field in the gap, and the physico-chemical properties of the liquid.

Streamer propagation phenomena in dielectric liquids are governed by both electronic and gaseous mechanisms. The former dominates when the energy injected in the medium is very important and/or in presence of halogens or aromatic molecules in the liquid. This is supported by the following facts: (i) the strong influence of small concentrations of electronic scavenger or low ionization potential additives on the shape and velocity of streamers, the corresponding current and emitted light, and the spectroscopic analysis of the emitted light by streamers, which indicate the presence of electronic processes; (ii) the strong effect of the hydrostatic pressure on the initiation and propagation of streamers, and the corresponding currents and emitted light, which indicate that the physical nature of the streamers is gaseous, con-

firmed by chromatographic analysis of the dissolved gases due to discharges.

Continuing investigations should be oriented towards measurement of the conductivity of the streamers to expand on results reported and discussed in the literature. The estimation of the temperature and the pressure within the streamer may help to identify the nature of streamers. Systematic spectroscopic and chromatographic analyses in real time can give more information concerning the physico-chemical processes (ionization, dissociation, vaporization...) involved in streamer propagation.

Members of the Liquid Dielectrics Committee International Study Group who participated in this study and their affiliations are: A. Beroual, Ecole Centrale de Lyon, CEGELY-CNRS, Ecully, France; M. Zahn, Massachusetts Institute of Technology, Cambridge, Massachusetts, USA; A. Badent, K. Kist, and A.J. Schwabe, the University of Karlsruhe, Germany; H. Yamashita and K. Yamazawa, Keio University, Yokohama, Japan; M. Danikas, Democritus University of Thrace, Xanthi, Greece; W.G. Chadband, Salford University, Salford, UK; and Y. Torshin, All-Russian Electrotechnical Institute, Moscow, Russia. The corresponding author, A. Beroual, may be reached at CEGELY - Ecole Centrale de Lyon, B.P. 163, 69131 Ecully Cedex, France.

REFERENCES

1. R.E. Hebner, "Measurements of Electrical Breakdown in Liquids," in *The Liquid State and its Electrical Properties*, E.E. Kunhardt, L.G. Christophoreau, and L.H. Luessen, Eds., Plenum Press, New York, pp. 519-537, 1988.
2. A. Badent, K. Kist and A.J. Schwab, "Voltage Dependence of Prebreakdown Phenomena in Insulating Oil," *Conference Record of the IEEE International Symposium on Electrical Insulation*, Pittsburg, PA, USA, June 5-8, 1994, pp. 414-417.
3. Yu; V. Torshin, "On the Existence of the Leader Discharges in Mineral Oil," *IEEE Trans. on Dielec. and Electr. Insul.*, Vol. 2, pp. 167-179, 1995.
4. J.C. Devins, S.J. Rzad and R.J. Schwabe, "Breakdown and Prebreakdown Phenomena in Liquids," *J. Appl. Phys.*, Vol. 52 (7), pp. 4531-4545, 1981.
5. A. Beroual and R. Tobazeon, "Prebreakdown Phenomena in Liquid Dielectrics," *IEEE Trans. on Electr. Insul.*, Vol. 21, pp. 613-627, 1986.
6. H. Yamashita and H. Amano, "Prebreakdown Phenomena in Hydrocarbon Liquids," *IEEE Trans. Electr. Insul.*, Vol. 23, pp. 739-750, 1988.

7. H. Yamada, T. Murakami, K. Kusano and T. Sato, "Positive Streamer Propagation and Breakdown Time Lag in Cyclohexane under Microsecond Rectangular Pulse Voltage," *Conf. Rec. of the 10th Int. Conf. on Cond. and Breakd. in Diel. Liq.*, IEEE No. 90CH2812-6, pp. 410-414, 1990.
8. H. Yamada, T. Murakami, K. Kusano, T. Fujiwara and T. Sato, "Positive Streamer in Cyclohexane under Microsecond Pulse Voltage," *Transactions on Electrical Insulation*, Vol. 26, pp. 708-714, 1991.
9. A. Beroual, "Prebreakdown Phenomena in Transformer Oil Under Step Voltages," *Archiwum Elektrotechn.*, 1/4, pp. 57-64, 1992.
10. Y. Kamata and Y. Kako, "Flashover Characteristics of Extremely Long Gaps in Transformer Oil under Non-uniform Field Conditions," *IEEE Trans. on Electr. Insul.*, Vol. 15, 1980, pp. 18-26.
11. A. Beroual, "Electronic Processes and Streamer Phenomena in Liquid Dielectrics," *Arch. Electrical Engineering*, No. 84, pp. 579-592, 1995.
12. R.E. Hebner, E.F. Kelley, E.O. Forster, and G.J. Fitzpatrick, "Observation of Prebreakdown and Breakdown Phenomena in Liquid Hydrocarbons Non-uniform Field Conditions," *IEEE Trans. Electr. Insul.*, EI-20, 2, pp. 281-292, 1985.
13. A. Beroual and R. Tobazeon, "Effects of Hydrostatic Pressure on the Prebreakdown Phenomena in Liquid Dielectrics," *C. R. Acad. Sciences, Paris*, t. 303, No 12, pp. 1081-1084, 1986.
14. A. Beroual, "Electronic and Gaseous Processes in the Prebreakdown Phenomena of Dielectric Liquids," *J. Appl. Phys.*, 73 (9), pp. 4528-4533, 1993.
15. K.N. Mathes and T.O. Rouse, "Influence of Aromatic Compounds in Oil on Pirelli Gassing and Impulse Surge Breakdown," *Ann. Rep., Conf. on Electr. Insul. and Dielect. Phenomena*, NAS - NRC, pp. 129-140, 1975.
16. A. Beroual and R. Tobazeon, "Propagation et Generation des Streamers dans les Dielectriques Liquides," *Rev. Phys. Appl.*, 22, pp. 1117-1123, 1987.
17. Y. Nakao, H. Itoh, S. Hoshino, Y. Sakai and H. Tagashira, "Effects of Additives on Prebreakdown Phenomena in n-Hexane," *IEEE Trans. on Diel. and Electr. Insul.*, Vol. 1, No. 3, pp. 383-390, 1994.
18. P. P. Wong and E. O. Forster, "The Dynamics of Electrical Breakdown in Liquid Hydrocarbons," *IEEE Trans. Electr. Insul.*, Vol. 17, pp. 203-220, 1982.
19. S. Sakamoto and H. Yamada, "Optical Study of Conduction and Breakdown in Dielectric Liquids," *IEEE Trans. Electr. Insul.*, Vol. 15, 3, pp. 171-181, 1980.
20. A. Beroual, "Spectral Analysis of Light Emitted by Streamers and Gas Chromatography in Liquid Dielectrics," *Jpn. J. Appl. Phys.*, Vol. 32, pp. 5615-5620, 1993.
21. A. Beroual, "Relationship Between Current, Charge and Propagation Velocity of Streamers in Dielectric Liquids," *Archiwum Elektrotechn.*, 1/4, pp. 45-56, 1992.
22. P.K. Watson, W.G. Chadband and M. Sadeghzadeh-Araghi, "The Role of Electrostatic and Hydrodynamic Forces in the Negative-Point Breakdown of Liquid Dielectrics," *IEEE Trans. on Electr. Insul.*, Vol.26, pp. 543-559, 1991.
23. W.G. Chadband and G.T. Wright, "A Prebreakdown Phenomena in the Liquid Dielectric Hexane," *Brit. J. Appl. Phys.*, Vol. 16, pp. 305-313, 1965.
24. P.K. Watson and W.G. Chadband, "The Dynamics of Pre-Breakdown Cavities in Viscous Silicone Fluids in Negative Point-Plane Gaps," *IEEE Trans. on Electr. Insul.*, Vol. 23, pp. 729-738, 1988.